Published in final edited form as:

*Vision Res*. 2015 May ; 110(0 0): 57–67. doi:10.1016/j.visres.2015.02.011.

# Speeding rod recovery improves temporal resolution in the retina

**Christopher R. Fortenbach**[a], **Christopher Kessler**[a], **Gabriel Peinado**[a], and **Marie E. Burns**[a,b,‡]

Christopher R. Fortenbach: cfortenbach@ucdavis.edu; Christopher Kessler: ckessler@ucdavis.edu; Gabriel Peinado: gpeinado@ucdavis.edu

[a]Center for Neuroscience, University of California Davis, Davis, California, United States of America 95616

[b]Depts. of Ophthalmology & Vision Science and Cell Biology and Human Anatomy, University of California Davis, Davis, California, United States of America 95616

## Abstract

The temporal resolution of the visual system progressively increases with light intensity. Under scotopic conditions, temporal resolution is relatively poor, and may be limited by both retinal and cortical processes. Rod photoresponses themselves are quite slow because of the slowly deactivating biochemical cascade needed for light transduction. Here, we have used a transgenic mouse line with faster than normal rod phototransduction deactivation (RGS9-overexpressors) to test whether rod signaling to second-order retinal neurons is rate-limited by phototransduction or by other mechanisms. We compared electrical responses of individual wild-type and RGS9-overexpressing (RGS9-ox) rods to steady illumination and found that RGS9-ox rods required 2-fold brighter light for comparable activation, owing to faster G-protein deactivation. When presented with flickering stimuli, RGS9-ox rods showed greater magnitude fluctuations around a given steady-state current amplitude. Likewise, *in vivo* electroretinography (ERG) and whole-cell recording from OFF-bipolar, rod bipolar, and horizontal cells of RGS9-ox mice displayed larger than normal magnitude flicker responses, demonstrating an improved ability to transmit frequency information across the rod synapse. Slow phototransduction recovery therefore limits synaptic transmission of increments and decrements of light intensity across the first retinal synapse in normal retinas, apparently sacrificing temporal responsiveness for greater overall sensitivity in ambient light.

### Keywords

retina; vision; bipolar; RGS9; rod; flicker



‡To whom correspondence should be addressed: meburns@ucdavis.edu; +1 (530) 752-1466.

## 1. Introduction

The visual system evolved to signal temporal contrast. In humans, the frequency at which changes in light intensity can no longer be discerned, called the critical flicker fusion frequency (CFF), increases with mean intensity. In dim light activating only rods, the CFF is relatively low (3–8 Hz); in brighter light that activates cones, higher frequencies (> 50 Hz) can be perceived (Hecht and Shlaer, 1936; Kelly, 1964; Conner and MacLeod, 1977). This dramatic difference in the temporal resolution of vision under scotopic versus photopic conditions may arise from differences in the photoresponse kinetics of rods and cones (Schnapf and Copenhagen, 1982; Bialek and Owen, 1990; Hess, 1990) or from the differences in temporal properties of circuits within the retina or beyond (Stockman et al., 1991; Snowden et al., 1995; Hess et al., 1996). Determining the site and specific biochemical process that limits the temporal resolution of rod vision has been difficult in part because of the concurrent activation of multiple parallel pathways in the retina (Wassle, 2004; Thoreson, 2007; Li et al., 2010).

Rods form direct chemical synapses with depolarizing rod bipolar cells ($DBC_R$s; primary rod pathway), and they form gap junctions with cones, which synapse with cone bipolar cells (secondary pathway; Tsukamoto et al., 2001; Deans et al., 2002). Infrequently, rods signal directly to both depolarizing (Pang et al., 2010) and hyperpolarizing, or OFF-, bipolar cells (HBCs; Tsukamoto et al., 2001; Li et al., 2010; Pang et al., 2012) to form the tertiary rod pathway. Paired whole cell recordings have shown that voltage changes in rods can be transmitted to HBCs nearly ten-fold faster than to their depolarizing counterparts (Li et al., 2010). These rod signaling pathways each vary in synaptic morphology and degree of convergence (Volgyi et al., 2004), as well as subtype-specific postsynaptic ion channels that further shape the time courses of bipolar cell responses (DeVries, 2000; Ivanova and Muller, 2006; Ichinose et al., 2014). Therefore it is unclear whether accelerating the time course of rod phototransduction signaling would affect the light responses of all, or indeed any, downstream bipolar cells receiving rod input.

To investigate this question, we examined retinal responses of mice with faster than normal rod phototransduction deactivation. 4-fold overexpression of the RGS9 complex (RGS9-ox) has little effect on the amplitude of the single photon response, but accelerates recovery and shortens the integration time of the flash response by speeding G-protein deactivation (Krispel et al., 2006; Gross and Burns, 2010). Using ERG and whole-cell recordings, we show that speeding rod deactivation decreases steady-state rod responses to continuous light but improves transmission of high-frequency information to second-order neurons, including both rod bipolar and OFF-bipolar cells. This indicates that slow rod recovery normally limits signaling across the first retinal synapse, sacrificing temporal responsiveness for greater overall sensitivity in ambient light.

## 2. Materials & Methods

### 2.1 Animals

All mice were cared for and handled with approval of UC Davis Institutional Animal Care and Use Committee and in accordance with NIH Guidelines. Mice were reared in 12h/12h

cyclic light and dark-adapted overnight prior to an experiment. All mice were between five and eleven weeks of age at the time of recording. RGS9-overexpressing mice were those described previously (Krispel et al., 2006), in which overexpression of a transgene encoding R9AP is driven by the rhodopsin promoter, resulting in over-expression of the entire RGS9 complex selectively in rods. The line used in this study corresponds to Line 2, which shows 4-fold RGS9 complex overexpression (Krispel et al., 2006). Control animals consisted of both wild-type (c57Bl6/J, Jackson Labs) and transgene-negative littermates.

### 2.2 Suction Electrode Recording

Under infrared light, mice were sacrificed by $CO_2$ narcosis and decapitation, and the retinas removed and stored in L-15 media supplemented with 10 mM dextrose on ice. Suction electrode recordings were performed at 34–36°C in bicarbonate-buffered Locke's as previously described (Krispel et al., 2006). While Ames medium was used for whole-cell recording to preserve inner retina health, rod response kinetics in Ames are considerably slower than when recorded in Locke's (Gross and Burns, 2010; Azevedo and Rieke, 2011). Locke's was therefore selected to be most conservative in assessing the impact of accelerate rod recovery of RGS9-ox rods.

Current responses were sampled at 200 Hz and low-pass filtered with an 8-pole Bessel filter set to a corner frequency of 30 Hz. The degree of dark current suppression by a given background intensity (2.9 to 6,100 R* $s^{-1}$) was measured by delivering a saturating flash (940 R* $s^{-1}$) after the onset of the steady light and comparing the amplitude of the evoked response to the amplitude of a saturating flash response in darkness. For flicker experiments, rods were stimulated with a square wave stimulus (100% contrast, 500 nm, 10 nm FWHM) with varied frequency (1–20 Hz). Wild-type and RGS9-ox rods were presented with mean flicker intensities of 180 and 430 R* $s^{-1}$, respectively.

### 2.3 Corneal Electroretinography (ERG)

Dark-adapted mice were set up for recording under very dim red light, anesthetized using 0.8–5% isoflurane (1 L/min), and maintained on a heated pad to help to regulate body temperature. Pupils were dilated with tropicamide, and a silver-wire loop electrode coated with methylcellulose solution was placed in electrical contact with the corneal surface. A subcutaneous electrode placed at the forehead served as reference. Differential signals were amplified and low-pass filtered at 1 kHz using a BMA-200 AC/DC Bioamplifier (CWE Incorporated). To determine the average degree of rod dark current suppression by a steady light, a saturating white xenon flash (L10211-04-04; Hamamatsu) was delivered on steady backgrounds produced by a high-power 500-nm LED (Thor Labs). The maximal a-wave amplitude on the background was then compared to the maximal a-wave amplitude in darkness. RGS9-overexpressing mice required a 2.6-fold brighter steady light to achieve the same steady-state level of a-wave amplitude suppression as wild-type mice. This was similar to the 2.3-fold intensity difference required while recording from individual rods (see Results).

Mice were presented with a sinusoidal stimulus (40% contrast) generated by a high-power 500-nm LED at varied intensities and frequencies (1–20 Hz). During a recording session,

each frequency and intensity was repeated a total of five times and those responses lacking significant electrical artifacts were subject to further analysis. ERG flicker responses were binned according to the degree of a-wave suppression at each mean flicker intensity (10%, 30%, 60% ± 5%) for subsequent Fourier analysis and averaging.

### 2.4 Whole-Cell Recording

Dark-adapted animals were sacrificed by cervical dislocation and decapitation, and eyecups with associated retinas were stored in the dark at 32°C in bicarbonate-buffered Ames medium (A1420, Sigma) equilibrated with 5% $CO_2$/95% $O_2$. Each retina was hemisected, then separated from the posterior pole and embedded in low-melting point agarose (A0701, Sigma). After solidifying, the agar block was cut into 200 μm slices using a vibrating microtome (Leica VT100S).

Methods and solutions for whole-cell recording were as described previously (Arman and Sampath, 2010). The internal solution contained (in mM): 125 K-aspartate, 10 KCl, 10 HEPES, 10 EGTA, 0.1 $CaCl_2$, 1 MgATP, 0.2 $Na_3GTP$, and 0.1 Alexa-488 (A10436, Life Technologies). All chemicals were purchased from Sigma (St. Louis, MO) unless otherwise indicated. For 7 of 14 OFF-bipolar cells, EGTA and $CaCl_2$ were substituted with (in mM) 5 EDTA and 0.5 $CaCl_2$. No significant difference between these two populations was observed as measured by peak current response ($p = 0.63$), peak voltage response ($p = 0.44$), resting potential ($p = 0.18$), or response latency ($p = 0.58$), so the populations were pooled during subsequent analysis.

The liquid junction potential between the internal solution and bicarbonate-buffered Ames (95% $O_2$, 5% $CO_2$) was measured via an agar salt bridge (4% agarose in 3 M KCl) at 37°C and found to be 5.7 ± 0.1 mV (n=3). This inherent offset was not taken into account during voltage-clamp experiments, but was used to correct the reported average resting potential values (Table 1).

Light-evoked current responses from rod bipolar, OFF-bipolar, and horizontal cells were recorded in voltage-clamp ($V_{holding}$ = −60mV) and current-clamp modes ($I_{holding}$ = 0 pA) in Ames medium bubbled with 95% $O_2$/5% $CO_2$ and warmed to 35–37°C. Flashes and sinusoidal flickering stimuli were presented at varied intensities and frequencies (100% contrast, 5–50 R* $rod^{-1}$ $s^{-1}$, 1–20 Hz) using a band-pass filtered LED (Thor Labs; 500 nm, 10 nm FWHM). Rundown occurred in the majority of $DBC_R$s and only those cells with a 15 pA or 5 mV maximal response were subject to further analysis. Latency was calculated as the time from the onset of a saturating flash (40 R* $rod^{-1}$ flash) to the time to reach half the maximal response amplitude during voltage-clamp recording.

Following recording, a subset of slices were fixed in 4% paraformaldehyde/PBS for 5–10 minutes at room temperature. Slices were blocked in 5% donkey serum for 1–2 hours and incubated overnight at 4°C in a solution containing 1X PBS, 0.5% BSA, 0.5% Triton X-100, and a 1:500 dilution of primary antibodies. Primary antibodies included: rabbit anti-Alexa Fluor 488 (A11094, Invitrogen) and mouse anti-calretinin (MAB1568, Millipore). After rinsing with PBS three times for five minutes each, the slices were incubated with secondary antibodies (dilution = 1:300). Secondary antibodies included: donkey anti-rabbit 488

(A21206, Invitrogen) and donkey anti-mouse 594 (A21203, Invitrogen). All $DBC_R$s had deep and confined axonal branching consistent with rod bipolar cells (Strettoi et al., 2010). OFF-bipolar (all subtypes were considered) and horizontal cells were identified based upon cell body location, axon terminal location, and the polarity of their electrical responses.

### 2.5 Light Calibrations

For suction electrode recordings, light from a tungsten-halogen bulb was attenuated with calibrated neutral density filters and band-pass filtered at either 500 nm or 520 nm (10 nm FWHM). Lamp power was determined using a calibrated silicon photodiode (UDT Instruments, Baltimore, MD) and converted into photon flux. A stepper motor controlled the shutter at frequencies specified by a command voltage output driven by custom written acquisition software in Igor Pro, and the duration and frequency of flicker confirmed by a photodiode mounted in the light path. For whole-cell recording, a 500 nm band-pass filtered (10 nm FWHM) high-power Luxeon white light-emitting diode (Thor Labs, Newton, NJ) was driven by a custom-made constant-current generator. The linearity of the output intensity ($R^2 > 0.99$) and frequency response of the LED was confirmed using a calibrated photodiode (UDT Instruments, Baltimore, MD). Light intensities were converted into the number of activated rhodopsins per rod per second (R* $rod^{-1}$ $s^{-1}$) by multiplying the photon flux (photons $\mu m^{-2}$ $s^{-1}$) by the effective collecting area of rods (0.5 $\mu m^2$; Field and Rieke, 2002).

For ERG recordings, retinal illumination was likely non-homogeneous and therefore accurate calibration was very difficult. The average degree of rod activation was estimated empirically by measuring the degree of a-wave suppression at different mean flicker intensities and using this percent suppression to average results across animals.

### 2.6 Analysis

The discrete Fourier transform (Igor Pro, Wavemetrics) was used to compute a magnitude spectrum for flicker responses collected between 2–5 seconds from stimulus onset. The fundamental magnitude at the stimulus frequency was divided by the maximal response amplitude to yield the normalized fundamental magnitude (NFM). Maximal responses could not be obtained from horizontal cells, which did not saturate even at very high intensities, presumably due to the contribution of cones; these cells were instead normalized using the amplitude obtained by a 40 R* $rod^{-1}$ flash. NFMs across cells at a given frequency and intensity were then averaged. For the ERG analysis, the NFM was determined for each repetition, and the normalized fundamental magnitudes were then averaged for each recording session and then across animals. Statistical significance as reported in the figures and Results was calculated using Student's *t*-test (two-tailed assuming equal variances; Microsoft Excel).

## 3. Results

### 3.1 Overexpressing the RGS9 complex in rods improves the rods' response to flicker

Because steady illumination induces several mechanisms of adaptation that decrease sensitivity and accelerate the kinetics of rod responses (Pugh et al., 1999; Fain et al., 2001),

we first needed to determine the intensity that would equally stimulate wild-type and RGS9-ox rods. Using suction electrodes, we recorded the responses of wild-type (WT) and RGS9-ox rods to steady light of varying intensities (Figure 1A). At each given light intensity, the steady-state responses of RGS9-ox rods were smaller than those of WT rods, due to faster than normal G-protein deactivation and thus lower steady-state levels of phosphodiesterase (PDE) activation. As a result, the steady-state response-intensity relationship for RGS9-ox rods was shifted to the right of that of WT rods (Figure 1B). On average, a 2.3-fold brighter intensity was needed to elicit a half-maximal response in RGS9-ox rods, consistent with the roughly 2-fold shorter integration time of RGS9-ox dim flash responses (Gross and Burns, 2010). Thus, in order for WT and RGS9-ox rods to have equivalent levels of intracellular calcium with comparable calcium-dependent adaptation mechanisms engaged, RGS9-ox rods require a 2-fold brighter intensity than WT rods (referred to hereafter as an equivalent intensity).

To assess the abilities of rods to signal changes in illumination, we presented flickering light (100% contrast, 1–20 Hz) at intensities producing comparable dark current suppression in WT and RGS9-ox rods, and recorded the resulting changes in outer segment currents (Figure 1C). Fourier analysis was used to extract the magnitude of the response fluctuations at each stimulus frequency (Figure 1D). At low frequencies of flicker (1–8 Hz) about a mean intensity of 180–430 R* $s^{-1}$ (39% dark current suppression), RGS9-ox rods showed greater amplitude current modulation than WT rods (Figure 1C–D; $p = 0.00038$, 0.00039, 0.011, and 0.021 for 1, 3, 5, and 8 Hz, respectively), with the greatest difference apparent at 3 Hz. At higher frequencies (10–15 Hz), the current modulation magnitudes of the two populations became indistinguishable (Figure 1C–D; $p > 0.05$).

These results show that speeding the rate-limiting step for rod recovery improves the ability of the outer segment to signal fluctuations in light intensity. If the kinetics of the rod outer segment photoresponse limits the temporal resolution of the visual system under scotopic conditions, the improved ability to follow flicker in the RGS9-ox rod should be successfully transmitted across the first retinal synapse. We therefore turned to electroretinography as a first step in evaluating the consequences of faster rod responses on retinal circuit function.

### 3.2 Improved ERG flicker response in RGS9-ox retinas

Electroretinography (ERG) measures light-evoked changes in electrical potential across the retina *in vivo*. Under scotopic conditions, these voltage changes are dominated by the summed responses of bipolar cells (Stockton and Slaughter, 1989; Abd-El-Barr et al., 2009). To examine the consequences of greater rod flicker modulation on the corneal ERG, a sinusoidally modulating stimulus (40% contrast) was presented at light intensities producing equivalent rod steady-state activation, as measured by the fractional suppression of the a-wave component of the ERG (see Materials & Methods; Pugh Jr et al., 1998). At light intensities suppressing 8.6% of the maximal rod a-wave, the amplitude of the voltage modulations were largest for low frequencies and fell as the frequency increased (Figure 2A), similar to the behavior observed in individual rods. At this dim light intensity (estimated from Figure 1B to be an equivalent intensity of ~10–20 R* $rod^{-1}$ $s^{-1}$), ERGs of RGS9-ox mice showed greater voltage modulation than WT mice at 5 Hz ($p = 0.024$; Figure

2B). At higher light intensities that suppressed 30.5% of the maximal a-wave (~50–150 R* $rod^{-1}$ $s^{-1}$; Figure 1B), the overall degree of modulation observed in both the WT and RGS9-ox ERGs increased (Figure 2B), with the RGS9-ox magnitudes far exceeding those of WT mice from 5–15 Hz ($p = 0.035$, 0.021, 0.012, and 0.0010 for 5, 8, 10, and 15 Hz, respectively). As the intensity increased further (64% a-wave suppression or ~400–800 R* $rod^{-1}$ $s^{-1}$; Figure 2C), the magnitude of the fluctuations decreased and the difference between the RGS9-ox and WT mice disappeared presumably because rods, the only cell type overexpressing RGS9, were approaching saturation. Furthermore, cones begin responding to light at ~100 R* $rod^{-1}$ $s^{-1}$ (Naarendorp et al., 2010) and complicate comparisons between the two mouse lines as photopic conditions are approached.

These results suggest that acceleration of rod photoresponse recovery improves the ability of rods to signal rapid changes in intensity to the rest of the retina, and show that this ability depends strongly on light intensity. Because of the relative insensitivity of the ERG recordings to very dim intensities, and because the moderate and higher light intensities used here likely also produced concurrent cone activation that could reduce apparent differences between RGS9-ox and WT mice, we next performed whole-cell recording from acute retinal slices to further investigate the impact of accelerated rod recovery on rod-driven retinal neurons.

### 3.3 OFF-bipolar, rod bipolar, and horizontal cells signal higher frequency flicker in RGS9-ox retinas

Hyperpolarizing, or OFF-, bipolar cells display faster response kinetics than depolarizing, or ON-, bipolar cells (Li et al., 2010; Burkhardt, 2011) due to differences in both glutamate receptor type (Kim and Miller, 1993; Nakanishi, 1994; Gerber, 2003) and synaptic morphology (DeVries et al., 2006). Although direct chemical synapses between rods and HBCs are relatively infrequent (Tsukamoto et al., 2001), the faster response kinetics of HBCs persist regardless of whether driven by rod or cone input (Li et al., 2010). Thus, HBCs in principle should be best suited to faithfully follow the faster responses observed in RGS9-overexpressing rods. We therefore recorded flicker responses from individual voltage-clamped HBCs that were presented with a sinusoidal stimulus (100% contrast, 1–20 Hz) with average intensities between 5–50 R* $rod^{-1}$ $s^{-1}$ (Figure 3). At the dimmest light intensity, HBC responses of WT retinas showed greatest modulation in response to low frequency flicker, the magnitude of which decreased sharply at frequencies higher than 5 Hz (Figure 3A). At equivalent low levels of rod activation (WT, 5 R* $rod^{-1}$ $s^{-1}$; RGS9-ox, 10 R* $rod^{-1}$ $s^{-1}$), the HBCs of RGS9-ox retinas displayed higher magnitude modulation than those of WT retinas at 8 and 10 Hz ($p = 0.034$ and 0.031, respectively). At 5-fold brighter light intensities (Figure 3B; WT, 25 R* $rod^{-1}$ $s^{-1}$; RGS9-ox, 50 R* $rod^{-1}$ $s^{-1}$), the magnitude of the fluctuations increased in both lines of mice, but HBCs of the RGS9-overexpressor again showed greater magnitude modulation, which reached statistical significance at 8 Hz ($p = 0.035$).

We also recorded from HBCs in voltage-following (current-clamp) mode, which allows for participation of voltage-sensitive currents. Overall, the magnitude of the HBC flicker responses in current clamp were larger in both WT and RGS9-ox retinas, suggesting that

voltage-sensitive currents amplify signaling. Although the differences between the WT and RGS9-ox retinas were smaller, the HBCs of the RGS9-ox retina continued to outperform those of the WT retina between 5 and 10 Hz ($p = 0.013–0.042$). Together, these results show that rod signaling to HBCs is indeed limited by slow rod recovery.

This finding then led us to ask whether depolarizing rod bipolar cells, which are thought to be specialized for single photon detection at the expense of temporal performance (Field and Rieke, 2002), might also show improved flicker modulation at dim light intensities. At the dimmest equivalent intensities (WT, 5 R* $rod^{-1}$ $s^{-1}$; RGS9-ox, 10 R* $rod^{-1}$ $s^{-1}$), $DBC_R$s were broadly tuned, displaying a gradual decrease in modulation amplitude as the flicker frequency increased (Figure 4A). Surprisingly, $DBC_R$s in the RGS9-ox background displayed a greater ability to follow flicker (reaching statistical significance for 8 Hz, $p = 0.034$) even at these modest intensities. With a 5-fold brighter stimulus, the magnitude of the responses increased dramatically and the flicker responses became more low-pass in nature, falling off steeply at frequencies above 8 Hz (Figure 4B); this is consistent with previous reports for rod-driven visually-guided behavior in mice (Umino et al., 2008; Umino et al., 2012). At this intensity, $DBC_R$s in the RGS9-ox background better followed flicker at both 5 and 8 Hz ($p = 0.00040$ and 0.011, respectively) and when voltage-sensitive conductances were freely allowed to change, the differences became even more evident (5, 8, 10 Hz; $p = 0.0021$, 0.0017, and 0.022, respectively).

The improvement in the temporal responsivity of bipolar cells in the RGS9-ox retina demonstrates that under normal physiological conditions, slow rod recovery limits the ability to convey rapid changes in illumination to these cells. In addition to rod bipolar cells, rods form invaginating synapses with horizontal cells, which play a critical role in establishing surround inhibition (Wassle, 2004), and shape the responses of both rods and cones (Thoreson et al., 2008; Trumpler et al., 2008). Similar to what had been observed in both sets of bipolar recordings, horizontal flicker responses fell in magnitude at higher frequencies, which became more pronounced at brighter intensities (Figure 5). Horizontal cells of RGS9-ox retinas showed greater amplitude modulation at low frequencies (1–8 Hz) under both voltage-clamp and current-clamp conditions, and at both equivalent light intensities. Interestingly, the contribution of voltage-sensitive conductances to the horizontal cell flicker responses was negligible: the magnitudes of the fluctuations between current- and voltage-clamp conditions were comparable in both WT and RGS9-ox backgrounds (Figure 5).

## 4. Discussion

It has been known for nearly a century that the temporal resolution of the mammalian visual system improves dramatically as light intensity increases (Hecht and Shlaer, 1936), but the underlying cellular or circuit mechanisms that achieve this improvement or that limit temporal resolution have not been determined. Here we show that speeding up the phototransduction deactivation of rods improves the ability of rods, bipolar cells, and horizontal cells to signal flicker. Thus, rod recovery limits the rate at which increments and decrements of light intensity are transmitted to rod-driven bipolar cells in normal retinas. This supports the view that the limited temporal resolution of the visual system in dim light

may originate from the slow signaling within the rod outer segments themselves, rather than from voltage-sensitive channels or synaptic mechanisms.

### 4.1 Rod deactivation limits the rate of signal transduction across the first retinal synapse

Previous studies have demonstrated that the recovery phase of the rod photoresponse does not participate in shaping bipolar cell responses to dim flashes of light. For instance, rod outer segment current responses reach their peak in approximately 125 ms, a time at which the electrical responses of rod bipolar cells have nearly concluded (Armstrong-Gold and Rieke, 2003; Sampath et al., 2005). However, here we demonstrate that when signaling increments and decrements from a mean light intensity, deactivation of the G-protein, transducin, limits both the ability of a rod to encode these stimuli (Figure 1) and its ability to signal across the first retinal synapse (Figures 2–5).

Rods display bandpass filtering of visual signals (Detwiler et al., 1978; Owen and Torre, 1983; Baylor et al., 1984) resulting, in part, from the attenuation of low frequency signals by hyperpolarization-activated cyclic nucleotide-gated (HCN1) channels (Owen and Torre, 1983; Barrow and Wu, 2009; Della Santina et al., 2012). The roll-off observed at frequencies above 4 Hz is consistent with the wild type rod's dominant time constant of recovery ($\tau_D$ = 246 ms; Krispel et al., 2006) and here we provide direct evidence that this attenuation of high frequency stimuli is the result of slow deactivation of the phototransduction cascade (Figure 1D). The three-fold acceleration in rod recovery in RGS9-ox rods ($\tau_D$ = 80 ms; Krispel et al., 2006) accounts for the larger flicker amplitudes observed below 10 Hz, while at higher frequencies, the RGS9-ox rod flicker responses become largely indistinguishable from wild type.

OFF-bipolar and horizontal cells display significantly shorter response latencies than depolarizing bipolar cells in salamander retinas (Burkhardt et al., 2007), and indeed that was also the case in our recordings from the mouse retina (Table 1). This presumably arises due to differences in synaptic machinery (Kim and Miller, 1993; Nakanishi, 1994; Gerber, 2003) and rod signaling pathways, which were not distinguished here. Rod signaling through the primary pathway to rod bipolar cells demonstrates exquisite sensitivity but is commonly thought to display limited temporal performance (Stockman et al., 1991; Sampath, 2014). It is therefore all the more surprising that, rather than being limited by a slow postsynaptic mechanism such as bipolar cascade deactivation by RGS7/RGS11 (Cao et al., 2012), the temporal responsiveness of rod bipolar cells is limited instead by rod photoresponse recovery.

Recently, the impact of rod recovery on the temporal resolution of mouse vision was assessed by ERG and the oculomotor response assay (Umino et al., 2012) by comparing normal mice to those with faster (RGS9-ox) rod recovery. Under single photon counting conditions (~0.4 R* $rod^{-1}$ $s^{-1}$), WT and RGS9-ox mice displayed no difference in their responses to flicker measured by ERG or behaviorally. At this very dim light intensity, each rod transmits a sparse series of single photon responses, rather than reporting changes in luminance about a mean level. Given the limited role of rod recovery in signaling flashes to bipolar cells, it is unsurprising that overexpression of RGS9 does not significantly impact the temporal resolution of the visual system at these intensities. However, as we have shown

here, rod recovery plays a significant role at brighter intensities (> 5 R* rod$^{-1}$ s$^{-1}$) both in its ability to encode rapidly changing intensities and to signal to second-order neurons.

When making comparisons between wild-type and RGS9-ox retinas, it was important to select mean light intensities producing equivalent steady-state rod activation, which strongly affects the noise, dynamic range, and kinetics of rod responses. For instance, in steady light, the flash responses of rods become smaller and faster, primarily as a consequence of reduced intracellular calcium (Fain et al., 2001). To ensure that differing light-adapted states did not affect our comparisons between the two lines of mice, we needed to compensate for the faster G-protein deactivation in RGS9-ox rods by selecting intensities producing equivalent steady-state levels of phosphodiesterase (PDE) activity, equivalent changes in calcium and cGMP levels, and thus equivalent dark current suppression. Given that stimulus intensity can influence noise fluctuations in rod responses, we confirmed that the variance of a subset of $DBC_R$ responses were similar between WT and RGS9-ox retinas stimulated at equivalent intensities ($p = 0.29$ and 0.64 at the dim and bright intensities, respectively). Therefore, stimulating at equivalent intensities results in both comparable intracellular calcium levels and noise fluctuations, which allows for comparison of temporal properties between RGS9-ox and WT retinas.

Retinal flicker responses are also shaped by voltage-dependent currents (Tanimoto et al., 2012). Bipolar responses at most frequencies increased during current-clamp recording (Figures 3–4, 6), suggesting that additional voltage-activated currents help to shape the bipolar cells' temporal response properties. While the specific sources of these currents are beyond the scope of this study, determining the identities of these channels and their distributions among various bipolar cell subtypes in the future will help to reveal the mechanisms that shape the temporal response properties of parallel rod pathways within the retina.

### 4.2 Rod-driven responses in rod bipolar and OFF-bipolar cells have distinct temporal response properties

The parallel ON- and OFF- visual pathways of the retina convey responses of opposite polarities to the cortex. Asymmetries between these pathways have frequently been reported in ganglion cells, though how they arise is not fully understood (Schiller, 2010). Here we report the first direct comparison of mammalian OFF- and rod bipolar cell responses to flicker. At mean intensities as low as 5 R* rod$^{-1}$ s$^{-1}$, OFF-bipolar cells display greater changes in membrane current than rod bipolar cells, even at low stimulus frequencies (Figure 6A). Given that rod bipolar cells are known for exquisite sensitivity (Sampath, 2014), it was surprising that OFF-bipolar cells were better able to follow flicker at such dim intensities. At 5-fold brighter intensities, rod bipolar cells respond with greater current and voltage modulation at low frequencies while OFF-bipolar cells perform better at frequencies above 8 Hz (Figure 6B). Unlike $DBC_R$s, HBCs receive input via multiple pathways that also display differing temporal properties (Stockman et al., 1991), though little is known mechanistically about the identities and relative strengths of these inputs. While the specific pathways by which HBCs received rod input were not investigated here, the improved temporal performance of HBCs over DBCs may result, in part, from a difference in temporal

properties of these input pathways. This greater ability of OFF-bipolar cells to convey rapid flicker is qualitatively similar to photopic bipolar recordings in salamander (Burkhardt et al., 2007) and suggests that the different temporal properties of ON- and OFF-ganglion cells observed in mice (Pandarinath et al., 2010) could arise at the level of the bipolar cells.

In response to both photopic flicker (Burkhardt et al., 2007) and sinusoidal variation of rod voltage (Armstrong-Gold and Rieke, 2003), horizontal cells display larger amplitude fluctuations than both classes of bipolar cells in salamanders. At the scotopic intensities tested here, however, they responded with smaller amplitudes than rod bipolar and OFF-bipolar cells (Figure 6). Previous studies have shown that rods stimulate somatic light-responses in horizontal cells by signaling across photoreceptor gap junctions to cone pedicles, which in turn synapse with horizontal cells (Peichl and González-Soriano, 1994; Thoreson et al., 2008; Trumpler et al., 2008). Given the relative insensitivity of rod signaling to bipolar cells via this pathway (Sharpe and Stockman, 1999; Abd-El-Barr et al., 2009), this might account for the diminished temporal performance of horizontal cells at the stimulus intensities investigated here.

Under photopic conditions, the transfer function of salamander ON-bipolar cells is that of a bandpass filter with peak responses observed between 2–3 Hz (Burkhardt et al., 2007). This has also been observed indirectly in rod bipolar cells of mouse at mean intensities as low as 300 R* $rod^{-1}$ $s^{-1}$ (Ke et al., 2014). Our recordings from rod bipolar cells, which were performed at considerably lower intensities, did not display a decreased ability to follow low frequency stimuli, suggesting that this high-pass filtering might only arise at intensities above 25 R* $rod^{-1}$ $s^{-1}$.

### 4.3 Conclusions

Rods are capable of signaling at light intensities varying over five orders of magnitude (Naarendorp et al., 2010) and the impact of their recovery kinetics on vision changes with intensity. In dim, steady light near visual threshold, rods serve as single-photon detectors and transmit individual photoresponses to downstream bipolar cells. When signaling a sparse sequence of single photons, the amplitude of the responses, rather than their recovery, dictates transmission across the non-linear threshold to rod bipolar cells (Field and Rieke, 2002; Armstrong-Gold and Rieke, 2003). At brighter intensities (> 5 R* $rod^{-1}$ $s^{-1}$) when rods convey increments and decrements from a mean level of phototransduction activity, our results show that the deactivation of the G-protein cascade limits the rods' ability to signal across the first retinal synapse. This indicates that the slow rod primary pathway is principally limited by rod recovery, rather than a postsynaptic mechanism (Sharpe and Stockman, 1999). With increasing intensity, light adaptation decreases rod sensitivity and accelerates rod response kinetics, presumably permitting rod signaling pathways to convey faster temporal stimuli. This fall in sensitivity is critical in extending the intensities over which rods can signal, but occurs at intensities significantly above visual threshold. Although speeding the integration time of the rod response ~2-fold due to RGS9-overexpression can improve the temporal responsiveness of the rod bipolar pathway 2-fold (Figure 4B), this also results in a 2-fold reduction in rod sensitivity (Figure 1). Thus it seems

that rods have opted to maintain their exquisite sensitivity at the expense of an improvement in the rate of signal transduction across the first retinal synapse.

## Acknowledgements

This work was supported by National Eye Institute Grants R01-EY014047 (MEB) and T32-EY015387 (NEI UC Davis Vision Training Grant), and the UC Davis Physician Scientist Training Program (CRF). We thank Megan Tillman for participation with ERG experiments and Edward N. Pugh. Jr. for frequent helpful discussions.

## Abbreviations

| | |
|---|---|
| **RGS9** | regulator of G protein signaling-9 |
| **RGS9-ox** | RGS9-overexpressing |
| **ERG** | electroretinogram |
| **CFF** | critical fusion frequency |
| **$DBC_R$** | rod bipolar cell |
| **HBC** | hyperpolarizing bipolar cell |
| **NFM** | normalized fundamental magnitude |
| **WT** | wild-type |
| **PDE** | phosphodiesterase |
| **HCN** | hyperpolarization-activated cyclic nucleotide-gated |

## References

Abd-El-Barr MM, Pennesi ME, Saszik SM, Barrow AJ, Lem J, Bramblett DE, Paul DL, Frishman LJ, Wu SM. Genetic dissection of rod and cone pathways in the dark-adapted mouse retina. Journal of neurophysiology. 2009; 102:1945–1955. [PubMed: 19587322]

Arman AC, Sampath AP. Patch clamp recordings from mouse retinal neurons in a dark-adapted slice preparation. Journal of visualized experiments : JoVE. 2010

Armstrong-Gold CE, Rieke F. Bandpass filtering at the rod to second-order cell synapse in salamander (Ambystoma tigrinum) retina. The Journal of neuroscience : the official journal of the Society for Neuroscience. 2003; 23:3796–3806. [PubMed: 12736350]

Azevedo AW, Rieke F. Experimental protocols alter phototransduction: the implications for retinal processing at visual threshold. The Journal of neuroscience : the official journal of the Society for Neuroscience. 2011; 31:3670–3682. [PubMed: 21389222]

Barrow AJ, Wu SM. Low-conductance HCN1 ion channels augment the frequency response of rod and cone photoreceptors. The Journal of neuroscience : the official journal of the Society for Neuroscience. 2009; 29:5841–5853. [PubMed: 19420251]

Baylor DA, Matthews G, Nunn BJ. Location and function of voltage-sensitive conductances in retinal rods of the salamander, Ambystoma tigrinum. The Journal of Physiology. 1984; 354:203–223. [PubMed: 6481634]

Bialek W, Owen WG. Temporal filtering in retinal bipolar cells. Elements of an optimal computation? Biophysical journal. 1990; 58:1227–1233.

Burkhardt DA. Contrast processing by ON and OFF bipolar cells. Visual neuroscience. 2011; 28:69–75. [PubMed: 21092350]

Burkhardt DA, Fahey PK, Sikora MA. Retinal bipolar cells: temporal filtering of signals from cone photoreceptors. Visual neuroscience. 2007; 24:765–774. [PubMed: 18093365]

Cao Y, Pahlberg J, Sarria I, Kamasawa N, Sampath AP, Martemyanov KA. Regulators of G protein signaling RGS7 and RGS11 determine the onset of the light response in ON bipolar neurons. Proceedings of the National Academy of Sciences of the United States of America. 2012; 109:7905–7910. [PubMed: 22547806]

Conner JD, MacLeod DI. Rod photoreceptors detect rapid flicker. Science. 1977; 195:698–699. [PubMed: 841308]

Deans MR, Volgyi B, Goodenough DA, Bloomfield SA, Paul DL. Connexin36 is essential for transmission of rod-mediated visual signals in the mammalian retina. Neuron. 2002; 36:703–712. [PubMed: 12441058]

Della Santina L, Piano I, Cangiano L, Caputo A, Ludwig A, Cervetto L, Gargini C. Processing of retinal signals in normal and HCN deficient mice. PloS one. 2012; 7:e29812. [PubMed: 22279546]

Detwiler PB, Hodgkin A, McNaughton P. A surprising property of electrical spread in the network of rods in the turtle's retina. Nature. 1978; 274:562–565. [PubMed: 672987]

DeVries SH. Bipolar cells use kainate and AMPA receptors to filter visual information into separate channels. Neuron. 2000; 28:847–856. [PubMed: 11163271]

DeVries SH, Li W, Saszik S. Parallel processing in two transmitter microenvironments at the cone photoreceptor synapse. Neuron. 2006; 50:735–748. [PubMed: 16731512]

Fain GL, Matthews HR, Cornwall MC, Koutalos Y. Adaptation in vertebrate photoreceptors. Physiological reviews. 2001; 81:117–151. [PubMed: 11152756]

Field GD, Rieke F. Nonlinear signal transfer from mouse rods to bipolar cells and implications for visual sensitivity. Neuron. 2002; 34:773–785. [PubMed: 12062023]

Gerber U. Metabotropic glutamate receptors in vertebrate retina. Documenta ophthalmologica Advances in ophthalmology. 2003; 106:83–87. [PubMed: 12675489]

Gross OP, Burns ME. Control of rhodopsin's active lifetime by arrestin-1 expression in mammalian rods. The Journal of neuroscience : the official journal of the Society for Neuroscience. 2010; 30:3450–3457. [PubMed: 20203204]

Hecht S, Shlaer S. Intermittent Stimulation by Light : V. The Relation between Intensity and Critical Frequency for Different Parts of the Spectrum. J Gen Physiol. 1936; 19:965–977. [PubMed: 19872976]

Hess, RF. Rod-mediated vision: role of post-receptoral filters. In: Hess, RF.; Sharpe, LT.; Nordby, K., editors. Night Vision: Basic, Clinical and Applied Aspects. Cambridge University Press; 1990. p. 3-47.

Hess RF, Waugh SJ, Nordby K. Rod temporal channels. Vision Res. 1996; 36:613–619. [PubMed: 8855005]

Ichinose T, Fyk-Kolodziej B, Cohn J. Roles of ON cone bipolar cell subtypes in temporal coding in the mouse retina. The Journal of Neuroscience. 2014; 34:8761–8771. [PubMed: 24966376]

Ivanova E, Muller F. Retinal bipolar cell types differ in their inventory of ion channels. Visual neuroscience. 2006; 23:143–154. [PubMed: 16638168]

Ke JB, Wang YV, Borghuis BG, Cembrowski MS, Riecke H, Kath WL, Demb JB, Singer JH. Adaptation to background light enables contrast coding at rod bipolar cell synapses. Neuron. 2014; 81:388–401. [PubMed: 24373883]

Kelly DH. Sine Waves and Flicker Fusion. Documenta ophthalmologica Advances in ophthalmology. 1964; 18:16–35. [PubMed: 14217806]

Kim HG, Miller RF. Properties of synaptic transmission from photoreceptors to bipolar cells in the mudpuppy retina. Journal of neurophysiology. 1993; 69:352–360. [PubMed: 8384660]

Krispel CM, Chen D, Melling N, Chen YJ, Martemyanov KA, Quillinan N, Arshavsky VY, Wensel TG, Chen CK, Burns ME. RGS expression rate-limits recovery of rod photoresponses. Neuron. 2006; 51:409–416. [PubMed: 16908407]

Li W, Chen S, DeVries SH. A fast rod photoreceptor signaling pathway in the mammalian retina. Nature neuroscience. 2010; 13:414–416.

Naarendorp F, Esdaille TM, Banden SM, Andrews-Labenski J, Gross OP, Pugh EN Jr. Dark light, rod saturation, and the absolute and incremental sensitivity of mouse cone vision. The Journal of neuroscience : the official journal of the Society for Neuroscience. 2010; 30:12495–12507. [PubMed: 20844144]

Nakanishi S. Metabotropic glutamate receptors: synaptic transmission, modulation, and plasticity. Neuron. 1994; 13:1031. [PubMed: 7946343]

Owen W, Torre V. High-pass filtering of small signals by retinal rods. Ionic studies. Biophysical journal. 1983; 41:325–339. [PubMed: 6404324]

Pandarinath C, Victor JD, Nirenberg S. Symmetry breakdown in the ON and OFF pathways of the retina at night: functional implications. The Journal of neuroscience : the official journal of the Society for Neuroscience. 2010; 30:10006–10014. [PubMed: 20668185]

Pang JJ, Gao F, Paul DL, Wu SM. Rod, M-cone and M/S-cone inputs to hyperpolarizing bipolar cells in the mouse retina. J Physiol. 2012; 590:845–854. [PubMed: 22219344]

Pang JJ, Gao F, Lem J, Bramblett DE, Paul DL, Wu SM. Direct rod input to cone BCs and direct cone input to rod BCs challenge the traditional view of mammalian BC circuitry. Proceedings of the National Academy of Sciences of the United States of America. 2010; 107:395–400. [PubMed: 20018684]

Peichl L, González-Soriano J. Morphological types of horizontal cell in rodent retinae: a comparison of rat, mouse, gerbil, and guinea pig. Visual neuroscience. 1994; 11:501–517. [PubMed: 8038125]

Pugh EN Jr, Nikonov S, Lamb TD. Molecular mechanisms of vertebrate photoreceptor light adaptation. Curr Opin Neurobiol. 1999; 9:410–418. [PubMed: 10448166]

Pugh, E., Jr; Falsini, B.; Lyubarsky, A. Photostasis and related phenomena. Springer; 1998. The origin of the major rod-and cone-driven components of the rodent electroretinogram and the effect of age and light-rearing history on the magnitude of these components; p. 93-128.

Sampath, AP. Information Transfer at the Rod-to-Rod Bipolar Cell Synapse. In: Werner, JSC.; L. M., editors. The New Visual Neurosciences. Cambridge: Massachusetts The MIT Press; 2014. p. 39-54.

Sampath AP, Strissel KJ, Elias R, Arshavsky VY, McGinnis JF, Chen J, Kawamura S, Rieke F, Hurley JB. Recoverin improves rod-mediated vision by enhancing signal transmission in the mouse retina. Neuron. 2005; 46:413–420. [PubMed: 15882641]

Schiller PH. Parallel information processing channels created in the retina. Proceedings of the National Academy of Sciences of the United States of America. 2010; 107:17087–17094. [PubMed: 20876118]

Schnapf JL, Copenhagen DR. Differences in the kinetics of rod and cone synaptic transmission. 1982

Sharpe LT, Stockman A. Rod pathways: the importance of seeing nothing. Trends Neurosci. 1999; 22:497–504. [PubMed: 10529817]

Snowden RJ, Hess RF, Waugh SJ. The processing of temporal modulation at different levels of retinal illuminance. Vision Res. 1995; 35:775–789. [PubMed: 7740769]

Stockman A, Sharpe LT, Zrenner E, Nordby K. Slow and fast pathways in the human rod visual system: electrophysiology and psychophysics. Journal of the Optical Society of America A, Optics and image science. 1991; 8:1657–1665.

Stockton RA, Slaughter MM. B-wave of the electroretinogram. A reflection of ON bipolar cell activity. J Gen Physiol. 1989; 93:101–122. [PubMed: 2915211]

Strettoi E, Novelli E, Mazzoni F, Barone I, Damiani D. Complexity of retinal cone bipolar cells. Progress in retinal and eye research. 2010; 29:272–283. [PubMed: 20362067]

Tanimoto N, Brombas A, Muller F, Seeliger MW. HCN1 channels significantly shape retinal photoresponses. Advances in experimental medicine and biology. 2012; 723:807–812. [PubMed: 22183410]

Thoreson WB. Kinetics of synaptic transmission at ribbon synapses of rods and cones. Molecular neurobiology. 2007; 36:205–223. [PubMed: 17955196]

Thoreson WB, Babai N, Bartoletti TM. Feedback from horizontal cells to rod photoreceptors in vertebrate retina. The Journal of neuroscience : the official journal of the Society for Neuroscience. 2008; 28:5691–5695. [PubMed: 18509030]

Trumpler J, Dedek K, Schubert T, de Sevilla Muller LP, Seeliger M, Humphries P, Biel M, Weiler R. Rod and cone contributions to horizontal cell light responses in the mouse retina. The Journal of neuroscience : the official journal of the Society for Neuroscience. 2008; 28:6818–6825. [PubMed: 18596157]

Tsukamoto Y, Morigiwa K, Ueda M, Sterling P. Microcircuits for night vision in mouse retina. The Journal of neuroscience : the official journal of the Society for Neuroscience. 2001; 21:8616–8623. [PubMed: 11606649]

Umino Y, Solessio E, Barlow RB. Speed, spatial, and temporal tuning of rod and cone vision in mouse. The Journal of neuroscience : the official journal of the Society for Neuroscience. 2008; 28:189–198. [PubMed: 18171936]

Umino Y, Herrmann R, Chen CK, Barlow RB, Arshavsky VY, Solessio E. The relationship between slow photoresponse recovery rate and temporal resolution of vision. The Journal of neuroscience : the official journal of the Society for Neuroscience. 2012; 32:14364–14373. [PubMed: 23055507]

Volgyi B, Deans MR, Paul DL, Bloomfield SA. Convergence and segregation of the multiple rod pathways in mammalian retina. The Journal of neuroscience : the official journal of the Society for Neuroscience. 2004; 24:11182–11192. [PubMed: 15590935]

Wassle H. Parallel processing in the mammalian retina. Nature reviews Neuroscience. 2004; 5:747–757.

- Acceleration of rod G protein deactivation increases response to flicker.
- Rod-driven OFF- bipolar responses signal higher frequencies than RBCs.
- Rod deactivation limits the temporal resolution of the first retinal synapse.

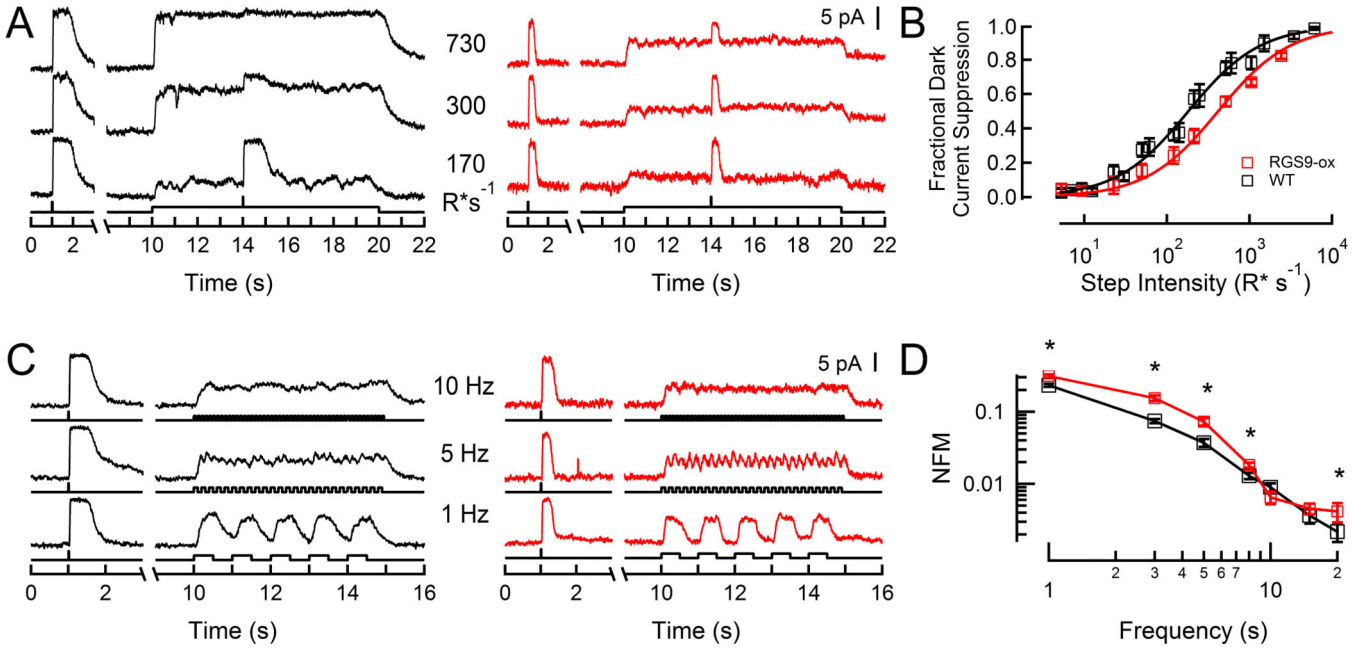


**Figure 1. Current responses of WT and RGS9-ox rods to flickering stimuli**

A: Representative responses of a WT rod (black) and an RGS9-ox rod (red) to steps of light. A saturating flash (940 R* flash$^{-1}$) was presented before and during each step to measure the remaining dark current.

B: Fraction of dark current suppressed as a function of intensity for a population of WT (black, n=4) and RGS9-ox (red, n=7) rods. Error bars represent SEM. Curves are Michaelis functions with half-saturating intensity values of 182 and 418 R* s$^{-1}$ for WT and RGS9-ox rods, respectively.

C: Representative flicker responses of a WT rod (black) and an RGS9-ox rod (red). Mean intensities were 180 and 430 R* s$^{-1}$ for WT and RGS9-ox, respectively.

D: Population average magnitude spectra at each test frequency for WT (black, n=7) and RGS9-ox (red, n=8) rods. A statistically significant difference was observed from 1–8 and 20 Hz ($p = 0.00038$, 0.00039, 0.011, 0.021, and 0.041, respectively). Throughout, error bars represent SEM. NFM: normalized fundamental magnitude. *$p < 0.05$

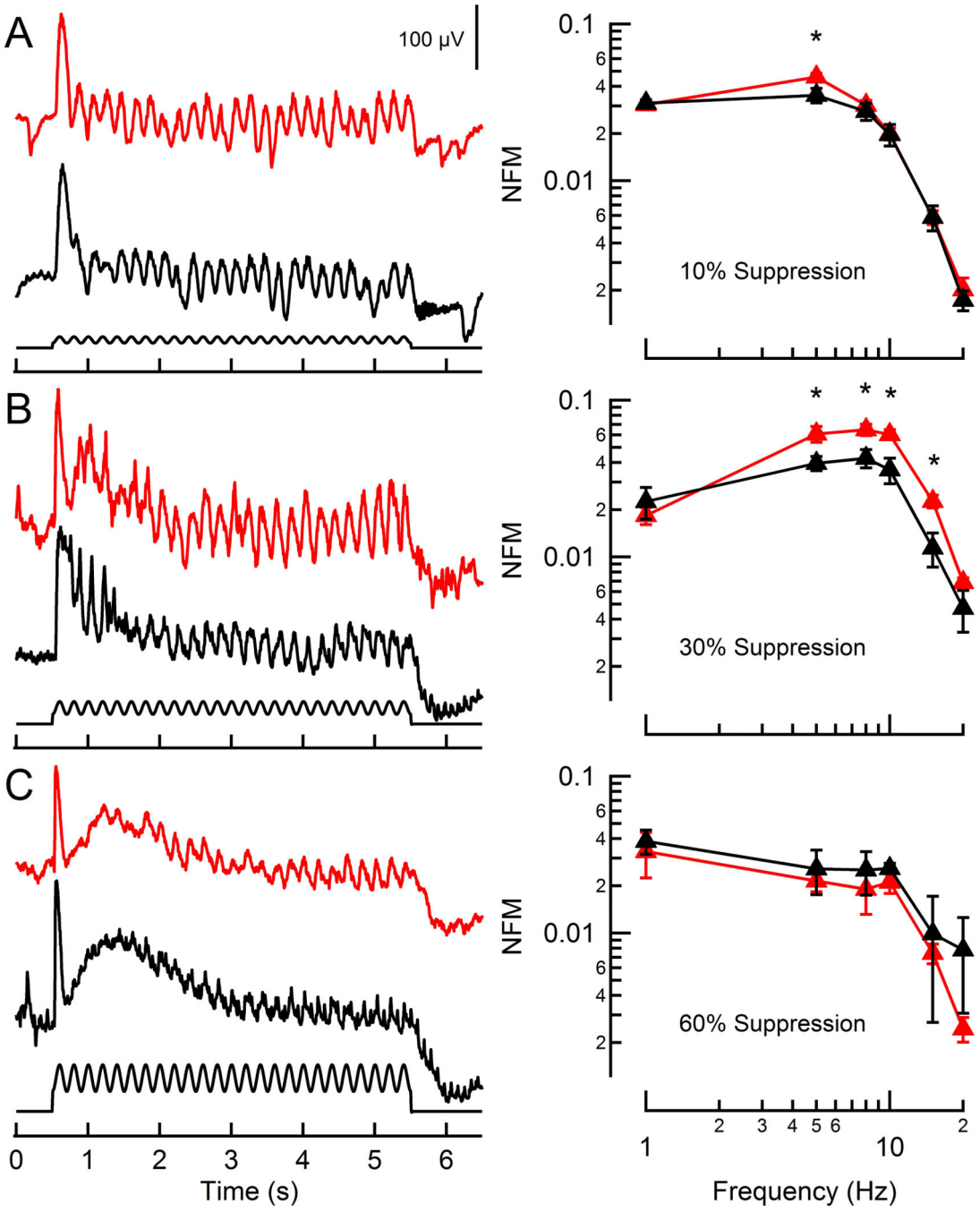


**Figure 2. ERG flicker responses of WT and RGS9-ox mice**

A–C (left): Representative corneal ERGs of WT (black) and RGS9-ox (red) mice in response to a 5 Hz flickering stimulus (500 nm, 40% contrast) at three intensities generating equivalent levels of rod activation, as measured by a-wave amplitude suppression. Each trace is the average of three recordings.

A–C (right): Population average magnitude spectra of ERGs at each fundamental test frequency, normalized by the maximal flash b-wave amplitudes. Each data point reflects between 2 and 6 determinations from a total of 12 RGS9-ox mice and 9 WT mice. A

statistically significant difference was observed at 5 Hz for the lowest intensity (A: $p = 0.024$) and from 5–15 Hz at the intermediate intensity (B: $p = 0.035$, 0.021, 0.012, and 0.0010, respectively). Error bars represent SEM. NFM: normalized fundamental magnitude. *$p < 0.05$

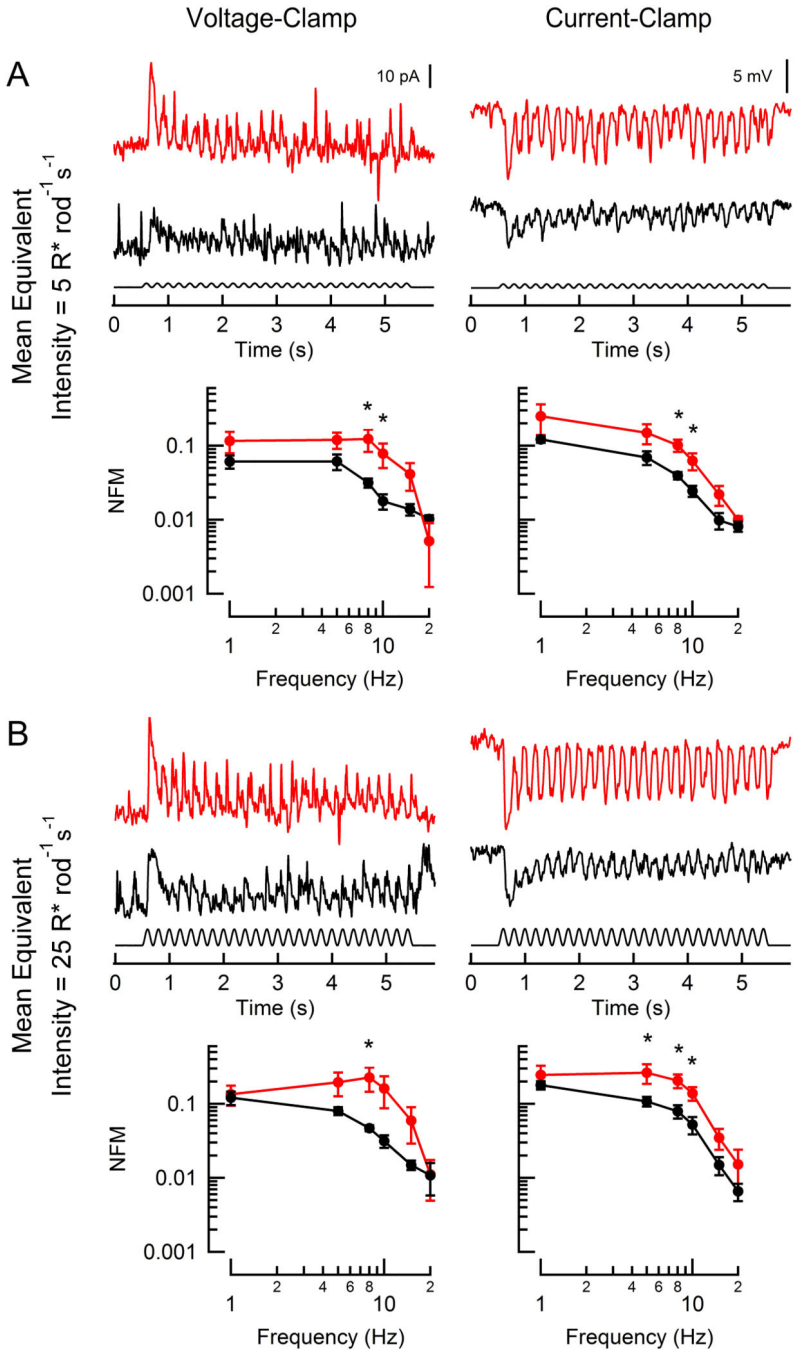


**Figure 3. Responses of rod-driven HBCs to flicker**

Representative light-evoked current (left) and voltage (right) responses from two hyperpolarizing bipolar cells (red: RGS9-ox background; black: WT) to flicker (100% contrast; 5 Hz). WT and RGS9-ox slices were stimulated at intensities generating equivalent rod suppression (A: 5 and 10 R* $rod^{-1}$ $s^{-1}$; B: 25 and 50 R* $rod^{-1}$ $s^{-1}$). Population average magnitude spectra are plotted below each sample trace for each condition. Each data point reflects between 2 and 7 determinations from a total of 8 RGS9-ox and 6 WT HBCs. A statistically significant difference was observed at 5, 8, and 10 Hz (A, left: p = 0.034 and

0.031; A, right: p = 0.017 and 0.039; B, left: p = 0.035; B, right: p = 0.042, 0.013, and 0.017). Error bars represent SEM. NFM: normalized fundamental magnitude. *p < 0.05

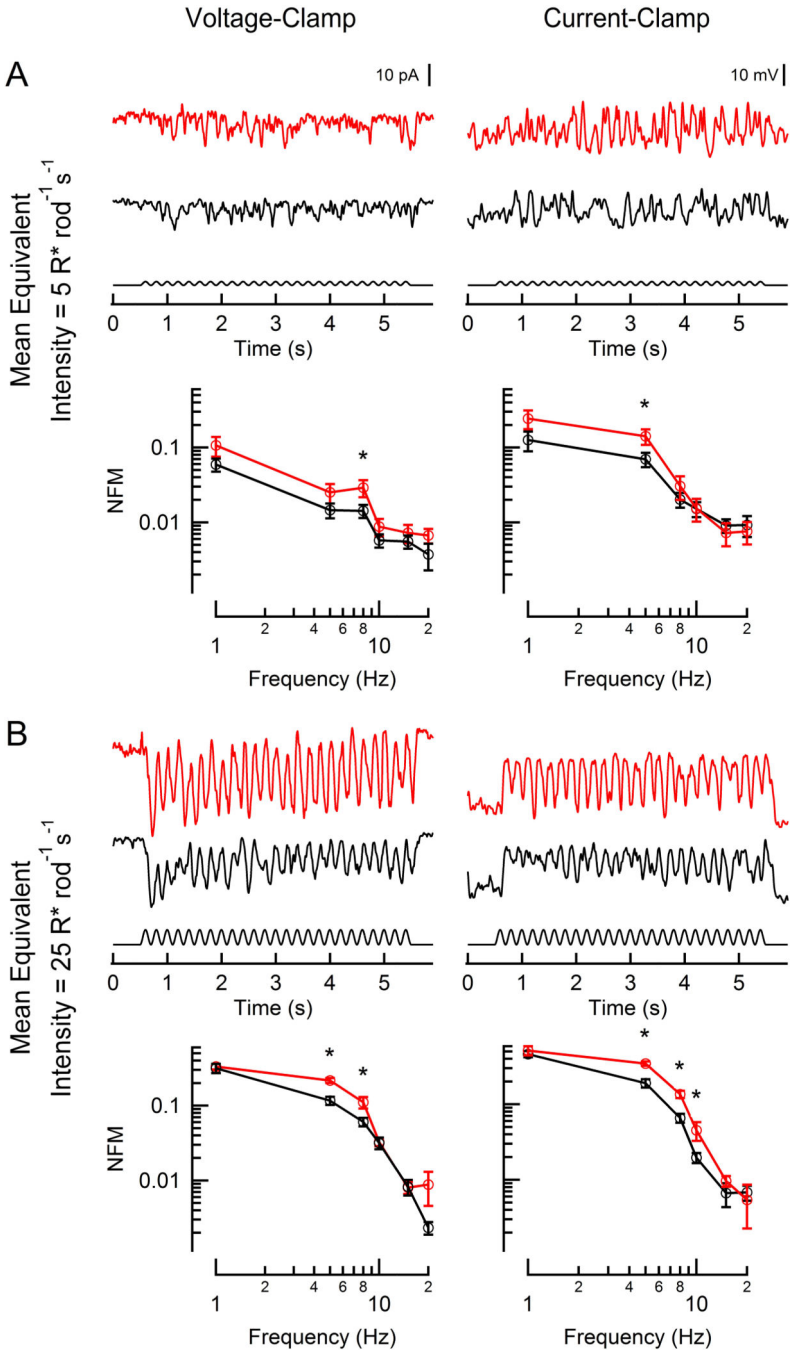


**Figure 4. Responses of rod-driven DBC$_R$s to flickering stimuli**

Representative light-evoked current (left) and voltage (right) responses from two rod bipolar cells (red: RGS9-ox background; black: WT) to flickering (100% contrast, 5 Hz). WT and RGS9-ox slices were stimulated at intensities generating equivalent rod suppression (A: 5 and 10 R* rod$^{-1}$ s$^{-1}$; B: 25 and 50 R* rod$^{-1}$ s$^{-1}$). Population average magnitude spectra are plotted below each sample trace for each condition. Each data point reflects between 3 and 15 determinations from a total of 7 RGS9-ox and 19 WT DBC$_R$s. A statistically significant difference was observed at 5 or 8 Hz at the lowest equivalent intensity (A, left: p =0.034; A,

right: p = 0.049) and between 5–10 Hz at the brighter equivalent intensity (B, left: p = 0.00040 and 0.011; B, right: p = 0.0021, 0.0017, 0.022). Error bars represent SEM. NFM: normalized fundamental magnitude. *p < 0.05

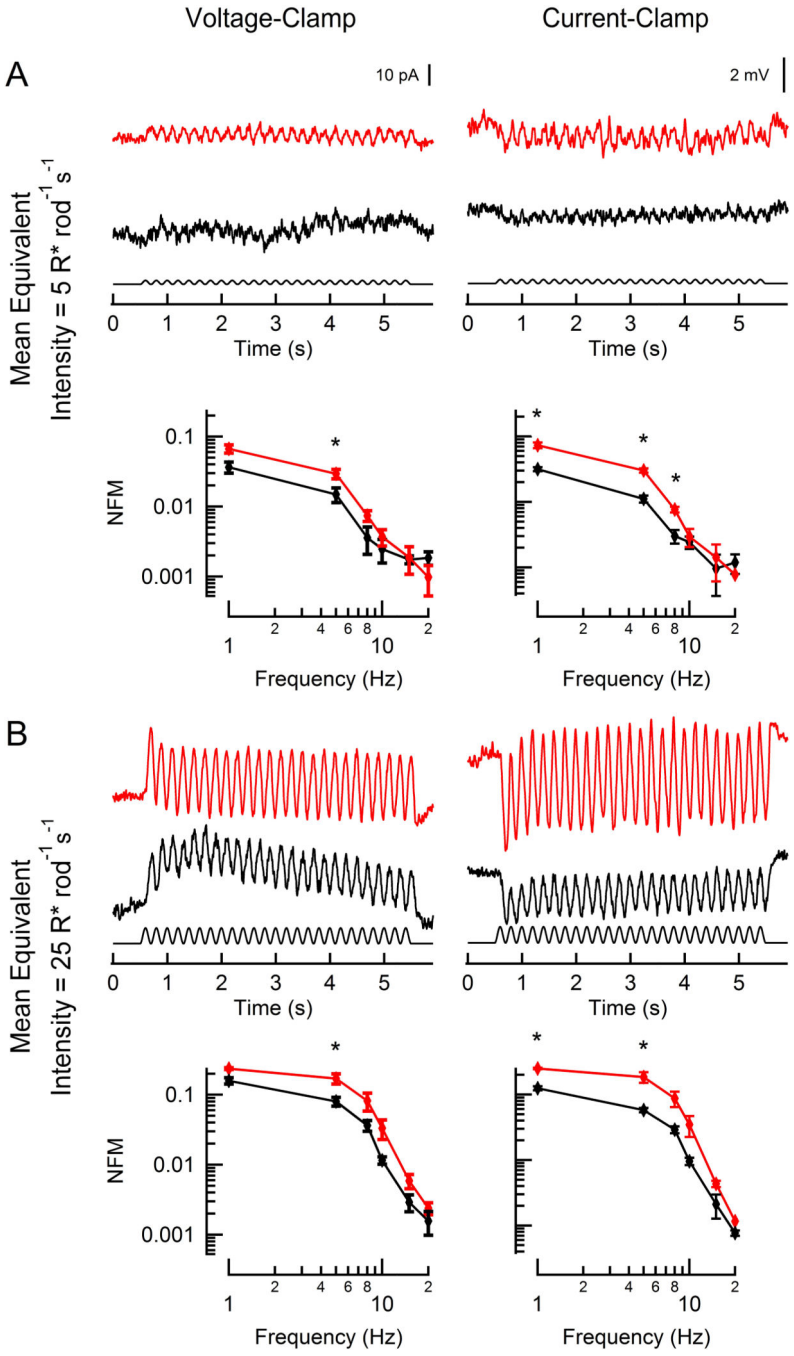


**Figure 5. Responses of rod-driven horizontal cells to flickering stimuli**

Representative light-evoked current (left) and voltage (right) responses from two horizontal cells (red: RGS9-ox background; black: WT) to a flickering stimulus (100% contrast, 5 Hz). WT and RGS9-ox slices were stimulated at intensities generating equivalent rod activity (A: 5 and 10 R* $rod^{-1}$ $s^{-1}$; B: 25 and 50 R* $rod^{-1}$ $s^{-1}$). Population average magnitude spectra are plotted below each sample trace for each condition. Each data point represents 3 determinations from 3 RGS9-ox and 3 WT horizontal cells. A statistically significant difference was observed between 1–8 Hz at the lowest equivalent intensity (A, left: p

=0.026; A, right: p = 0.0059, 0.0020, and 0.012) and between 1–5 Hz at the brighter equivalent intensity (B, left: p = 0.016; B, right: p = 0.00041 and 0.021). Error bars represent SEM. NFM: normalized fundamental magnitude. *p < 0.05

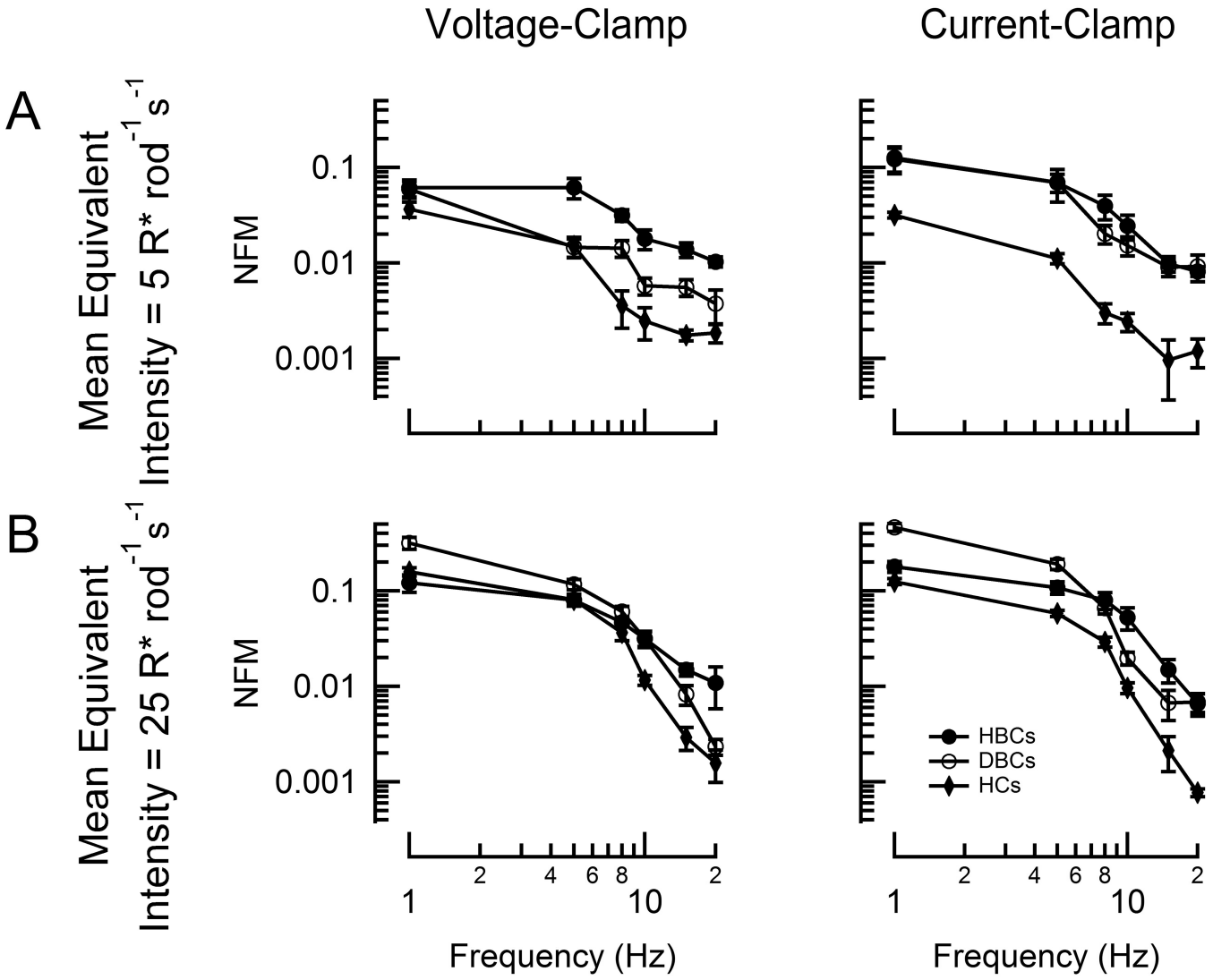


**Figure 6. OFF-bipolar cells are more adept than rod bipolar cells at signaling flicker in very dim light**

Population average magnitude spectra of current (left) and voltage (right) modulation at each test frequency for WT rod bipolar (open black circles), hyperpolarizing bipolar cells (closed black circles), and horizontal cells (HCs; closed black diamonds) at two mean stimulus intensities (A: 5 R* $rod^{-1}$ $s^{-1}$; B: 25 R* $rod^{-1}$ $s^{-1}$). Each data point reflects between 2 and 15 determinations from a total of 19 $DBC_R$s, 7 HBCs, and 3 HCs. Error bars represent SEM. NFM: normalized fundamental magnitude.

**Table 1**

Characteristics of Dark-Adapted ERG and Whole-Cell Responses in WT and RGS9-ox Mice

| | **A-wave$_{max}$ (μV)** | **B-wave$_{max}$ (μV)** | | **$R_{max}$ (pA)** | **$R_{max}$ (mV)** | **Series Resistance (MΩ)** | **Resting Potential (mV)** | **Latency (ms)** |
|---|---|---|---|---|---|---|---|---|
| | | | $DBC_R$ | −84.6 ± 17.5 (21) | 22.4 ± 2.5 (9) | 191.5 ± 36.3 (21) | −32.2 ± 3.4 (9) | 64.0 ± 3.9 (21) |
| Wild-Type | −390 ± 36.5 | 608 ± 64.3 | HBC | 76.4 ± 15.5 (7) | −21.9 ± 3.3 (6) | 288.0 ± 115.9 (5) | −34.2 ± 0.9 (6) | 48.4 ± 4.7 (7) |
| | | | HC | 255 ± 52.2 (3) | −19.0 ± 1.4 (3) | 56.8 ± 3.2 (2) | −41.5 ± 3.3 (3) | 42.5 ± 1.6 (3) |
| | | | $DBC_R$ | −66.5 ± 11.1 (7) | 26.7 ± 2.7 (5) | 129.9 ± 42.7 (7) | −34.9 ± 4.0 (5) | 58.9 ± 3.1 (7) |
| RGS9-ox | −438 ± 36.0 | 702 ± 51.2 | HBC | 87.7 ± 31.9 (7) | −13.2 ± 1.7 (4) | 367.6 ± 97.6 (5) | −37.0 ± 4.7 (5) | 42.8 ± 3.5 (3) |
| | | | HC | 346 ± 84.3 (3) | −19.4 ± 2.3 (3) | 91.7 ± 31.9 (3) | −35.8 ± 2.4 (3) | 44.7 ± 1.7 (3) |

$R_{max}$, maximal response amplitude; $DBC_R$, rod bipolar cell; HBC, hyperpolarizing bipolar cell; HC, horizontal cell